Three-body continuum spatial correlations in Borromean halo nuclei

B. V. Danilin
The Kurchatov Institute, 123182 Moscow, Russia

T. Rogde and J. S. Vaagen
SENTEF, Institute of Physics, University of Bergen, Norway

I. J. Thompson
Department of Physics, University of Surrey, Guildford GU2 7XH, United Kingdom

M. V. Zhukov
Department of Physics, Göteborg University and Chalmers University of Technology, Göteborg, Sweden

[RNBT (Russian-Nordic-British Theory) Collaboration]

Spatial correlations in the three-body continuum of Borromean (having no bound binary subsystems) three-body systems are discussed. The hyperspherical harmonics method is used to investigate low-lying resonances and the soft dipole mode in the two-neutron halo nucleus ^{6}He, which has only the $\alpha+n+n$ continuum for excitation energies below 13 MeV. The spatial correlations reveal characteristic structures for true three-body resonances, a moderate amplification in the interior region for above-barrier resonances and long-range correlations in the cases of three-body 1^- virtual and 0^+ continuum states.

I. INTRODUCTION

In this article we continue our explorations of spectra of Borromean halo nuclei, those having no bound binary subsystems. Within the hyperspherical harmonics (HH) method [1–3] we investigate spatial correlations in the three-body continuum. Our aim is to elucidate the physical nature and characteristic structures of true three-body resonances, and to identify long-range correlations in specific three-body states such as the soft dipole and monopole modes. We will examine three-body scattering amplitudes and the internal parts of calculated three-body continuum wave functions and graphically present their three-body correlations.

A variety of few-body methods have been used for *bound* states of Borromean nuclei, in a *core+n+n* cluster decomposition fully including three-body dynamics, but few are suitable for *continuum* analysis. The methods that have been applied to the ^{6}He continuum include, besides the HH method [1,2,4], the adiabatic hyperspherical method [5], the Gamow states (complex energy) method [6,5], the coordinate complex rotation method [7,8], algebraic version of the resonating group method [9], the harmonic oscillator representation of scattering equations [10], and analytic continuation in the coupling constant [11]. These methods show some common features such as compression of continuum spectra in comparison with shell-model-type expectations [2], and candidates for 2_2^+, 1^+, and 0^+ resonances in the energy interval $1-5$ MeV, although these states have not yet been distinguished experimentally.

Progress in exclusive experimental studies of the structure of the ^{6}He continua has recently been made, and also theoretically by considering the different aspects of the three-

body problem and its solution [2] based on the Schrödinger equation and the coordinate-space HH method. The relevant wave function (WF) is that for $3 \rightarrow 3$ scattering, which, although not directly measurable, has a role as final state of any reaction leading to the ^{6}He (or any Borromean) continuum. For example it was used for charge-exchange reactions and inelastic scattering in four-body distorted-wave Born approximation theory [12] and in electromagnetic dissociation [2]. Such reaction models are necessary for the full analysis of kinematically complete breakup of ^{6}He on heavy and light targets, as measured at GSI [13]. The experimental advances are discussed in recent reviews of experiments [14–16].

II. CORRELATIONS IN THE THREE-BODY CONTINUUM

A. Continuum structures

When two halo neutrons are interacting with a core at positive energies, three-body scattering theory is needed. The appendix describes briefly the normalized Jacobi spatial $\{\mathbf{x}, \mathbf{y}\}$ and momentum $\{\mathbf{k}_x, \mathbf{k}_y\}$ coordinates used to describe three-body dynamics, and defines plane waves and scattering waves in the three-body continuum. The free plane wave is defined to include the effect of antisymmetrization between the halo neutrons, henceforth referred to as the antisymmetrized plane wave (APW).

Generally the spatial structure of a scattering wave may have two distinct kinds of deviations of its internal part from that of the APW. The benchmark behavior is the case of a narrow three-body resonance, characterized by a strong amplification of the interior part of the WF in a compact region

69 024609-1

of mutual interaction. These resonances are often generated by a pocket in some of the diagonal HH potentials, which are hyperangular averaged sums of all the partial binary interactions plus corresponding three-body centrifugal barriers. Note that these barriers exist even if all binary angular momenta are equal to zero, in contrast to a two-body problem. Due to the large spatial overlap with the ground state in the region of resonant amplification, inelastic transitions to these resonances are very strong.

Another type of specific states are continuum structures arising from long-range effective interactions in the three-body system, having a range of the order of the sum of the scattering lengths in the binary subsystems. There is a physical analogy with the bound state Efimov effect [17], where a number of bound states and their spatial extension in a three-body system without binary bound states depends on ratio of the binary scattering length to the interaction radius. We will classify such structures as Efimov-like states. In general, this reflects the possibility of a third particle to "feel" the interaction of the two other particles at a distance up to the scattering length. When we deal with a Borromean two-neutron halo, the neutron-neutron s-wave interaction with scattering length ~ 16 fm is decisive for this effect, which resembles "continuum pairing" in the shell model and is responsible for the compression of continuum spectra near three-body threshold, as in the ^{6}He case [2].

There is then a large correlation distance due to long-living resonances or virtual (antibound) states in two-body subsystems propagating to large distances, and there may be no pronounced concentration of the wave function inside the region of interaction of all three particles, but rather a long-range spreading of correlations.

These features should be visible in specific details of three- and many-body "observables," especially in the spatial correlated densities to be shown. Such spatial densities proved to be very useful for the ground state representation of ^{6}He [3], and are in this paper generalized to continuum states.

Before presenting detailed correlation densities, we expand a little further on the general characteristics of resonances and other structures that may be expected in the three-body continuum.

In the two-body case the centrifugal and/or Coulomb barriers combined with an attractive internal part of potential can generate characteristic "narrow" (sub-barrier) and broad (above-barrier) resonances with significant peaks in the elastic cross section. Furthermore, a purely repulsive potential can also generate what are called barrier-top resonances, well known in nuclear quasimolecules [18]. The characteristic feature of a barrier-top resonance is a small resonance peak in the elastic cross section, while the interior norm exhibits a sharp resonant behavior [19], which can be seen in transitions.

In the three-body case, the coupled-channels problem sometimes has no explicit analogies with potential scattering, but after diagonalization of the potential and centrifugal matrices the lowest adiabatic terms give a rather similar physical picture (especially in the strong coupling case). For discussion in the momentum representation, see also Ref. [20].

Physically, in a three-body system there may exist long-living states of three types.

(I) The "true" narrow three-body resonance having an amplitude with the analytic form [21]

$$A \sim \frac{c}{E - (E_0 - i\Gamma_0/2)}, \tag{1}$$

where E_0 and Γ_0 are position and width of the resonance, respectively [for simplicity we omit the dependence of A on Ω_5^ρ and Ω_5^κ indicated in Eq. (A7)]. The most important feature of a true three-body resonance is that it is strongly present in lowest-K (hypermoment) configurations, and corresponds to three particles interacting close to each other. As a consequence, the hyperradial WF of Eq. (A5) has main components, which in the interaction region, have a characteristic resonance amplification whose energy dependence coincides with the asymptotic behavior of the WF expressed by the scattering amplitude Eq. (1), as familiar from two-body scattering. This spatial behavior can be represented by a factorized form

$$\psi_{K\gamma;K'\gamma'}(\rho;E) \sim C_{K\gamma;K'\gamma'}(E)\psi_{K\gamma}^R(\rho) \tag{2}$$

with

$$|C_{K\gamma;K'\gamma'}(E)|^2 = \frac{d_{K\gamma;K'\gamma'}}{(E - E_0)^2 + \Gamma_0^2/4}, \tag{3}$$

where $\psi_{K\gamma}^R(\rho)$ is the energy-independent form of the internal part of the scattering WF. In the two-body case, a coincidence of the resonant features of the scattering amplitude and the internal part of the WF is clear from the Lippman-Schwinger equation. It connects the scattering amplitude with the overlap of the scattering WF with the potential, which is concentrated in the region of interaction of the particles (internal part of scattering WF). In the three-body case the same connection follows qualitatively from a finite matrix analog of the Lippman-Schwinger equation, as was seen explicitly [22] in the case of the well-known 2_1^+ resonance in ^{6}He. The results of a transition amplitude calculation, comparing a quasibound resonance WF with the strict continuum WF, show rather good agreement [22].

Because of the concentration of a resonant WF in the three-body interaction region, the resonant WFs have large radial overlaps with the bound state, and the energy behavior of the transition amplitude (determined by short distances) therefore will be very close to that of the scattering amplitude (derived from the asymptotics i.e., large distances).

This conclusion also follows from a simple semirigorous argument from two-body scattering [23]. The time delay for a resonance is $2\hbar d\delta/dE$, where δ is the phase shift. The interaction region stores probability accumulated over this time, given by the probability current multiplied by the time delay,

$$J2\hbar\frac{d\delta}{dE} = \frac{1}{4}\frac{\hbar\kappa}{m}2\hbar\frac{d\delta}{dE}.$$

In the three-body coupled-channels case we may use

the resonant eigenphase δ_{res} (see, for example, Ref. [2] for ^{6}He) of the symmetric complex S matrix, which can be diagonalized via an unitary transform $S_{diag} = U^{-1} S U$ to S_{diag} which has unit-modulus elements $e^{2i\delta_l}$. The resonant eigenphase δ_{res} contains joint information about the effect of the resonance in each coupled channel, in the same way as in two-body problem. The change of probability in the interior region due to the mutual interactions can be estimated as the difference between the probabilities with and without interactions,

$$\sum_{K\gamma} \int_0^R (|\psi_{K\gamma,K'\gamma'}(\rho;E)|^2 - |\phi_{K\gamma}(\kappa\rho)|^2) d\rho \approx \frac{1}{4} \frac{\hbar\kappa}{m} 2\hbar \frac{d\delta_{res}}{dE},$$

where $\phi_{K\gamma}(\kappa\rho)$ is the plane wave radial wave function in Eq. (A4). The maximum in $d\delta_{res}/dE$ has to correspond to a maximum in $\int |\psi|^2 d\rho$, which is the internal norm already used in the analysis of resonances in the three-body continuum [2].

(II) There may be a trace of a two-body resonance or virtual state in the three-body system, even in absence of a true three-body resonance [21]. Here, however, there may be no rigorous analytic structure such as for (I). A rather general expression, in case of a long-living resonant state in a binary subsystem, which interacts only weakly with the third particle, is

$$A \sim \frac{c_\gamma(E)}{\epsilon - (\tilde{\epsilon} - i\tilde{\Gamma}/2)}. \tag{4}$$

Here ϵ is the part of the total energy E shared by the resonant subsystem and $\tilde{\epsilon} - i\tilde{\Gamma}/2 = \epsilon_0 + \Delta\epsilon - i(\tilde{\Gamma}_0/2 + \Delta\Gamma/2)$ with ϵ_0 and Γ_0 being the position and width of the binary resonance, respectively (without the presence of the third particle). The terms in $\Delta\epsilon$ and $\Delta\Gamma/2$ are the shift and additional width due to the coupling with the third particle, while $c_\gamma(E)$ is some smooth function of the total energy E. Physically this corresponds to a large correlation distance when the two particles in the binary resonance (being close to each other) are moving at a significant distance relative to the third.

(III) A third type of resonance can be created by distributed coupling between the hyperradial channels in absence of deep diagonal potentials, and is characterized by overall properties of the system such as the ratio of couplings, the diagonal potentials, and the number of channels. Physically, such a resonance could be interpreted as a parametric resonance arising from the quantum diffusion type transitions

with complex coefficients in channel space [24]. In any case, in coupled-channel problems, so-called "CC resonances" (see Ref. [25] illustrating the phenomenon in a two channels system) may be caused by large off-diagonal potential components, even if the diagonal potentials are small.

In this kind of resonance there could also be large scale spatial correlations because of virtual transitions to and from many strongly coupled channels with different internal angular momenta l_x, l_y. In such a case, none of these channels dominate, in contrast to resonance conditions (I) and (II), and transitions to channels with higher l_x, l_y correspond to spreading of correlations to larger distances.

B. Correlated spatial densities

A measure of spatial distribution in the three-body case is the correlated density in the relative coordinates $(\mathbf{r}_{ij}, \mathbf{r}_{(ij)k})$, which are distances between any two particles and between their center of mass and the third one. They are collinear with the normalized Jacobi coordinates $(\mathbf{x}_k, \mathbf{y}_k)$. For a bound state the correlated density gives the probability of two particles to be at distance $\mathbf{r}_{ij}$, while their center of mass is at a distance $\mathbf{r}_{(ij)k}$ from the third particle. Calculations for the ^{6}He ground state [26,3] revealed, in the cluster **T** basis, specific correlations such as "dineutron" and "cigar" configurations of the halo neutrons which are due to Pauli principle exclusion of the lowest s-motion and called Pauli focusing in Ref. [27].

In the continuum, for three-body states with definite JT and energy $E = \hbar^2 \kappa^2/2m$, we use the differential probability obtained from the full scattering WF of Eq. (A5) in the presence of the interactions,

$$dP^J(\mathbf{k}_x, \mathbf{k}_y, \mathbf{x}, \mathbf{y}) = \sum_M |\Psi_{\kappa JM}^T(\mathbf{x}, \mathbf{y}, \mathbf{k}_x, \mathbf{k}_y)|^2 d\mathbf{x} d\mathbf{y} \; d\mathbf{k}_x d\mathbf{k}_y. \tag{5}$$

We now average this probability density over the spatial $(\hat{\mathbf{x}}, \hat{\mathbf{y}})$ and momentum $(\hat{\mathbf{k}}_x, \hat{\mathbf{k}}_y)$ directions, and also over total spin S and hyperangle α_κ (which is a measure of distribution of the total energy E between the particles). Since

$$d\mathbf{x} d\mathbf{y} = a_{ijk} r_{ij}^2 dr_{ij} r_{(ij)k}^2 dr_{(ij)k} d\hat{\mathbf{x}} d\hat{\mathbf{y}} \tag{6}$$

and

$$d\mathbf{k}_x d\mathbf{k}_y = \kappa^5 \; d\kappa d\Omega_5^\kappa = m/\hbar^2 \kappa^4 dE d\Omega_5^\kappa, \tag{7}$$

we obtain after integration over $\hat{\mathbf{x}}, \hat{\mathbf{y}}$, and Ω_5^κ, the correlated density

$$p^J(E, r_{ij}, r_{(ij)k}) = \frac{dP^J(E, r_{ij}, r_{(ij)k})}{dr_{ij} dr_{(ij)k} dE} = a_{ijk}(m/\hbar^2) r_{ij}^2 r_{(ij)k}^2 \kappa^{-1} \rho^{-5} \sum_{KLSl_x l_y} \sum_{L'S'l_x' l_y'} \sum_{K'',K'} \psi_{K'\gamma',K\gamma}^J(\rho;E) \psi_{K''\gamma',K\gamma}^J(\rho;E)^*$$

$$\times N_{K'}^{l_x' l_y'} (\sin \alpha)^{l_x'} (\cos \alpha)^{l_y'} P_{(K'-l_x'-l_y')/2}^{l_x'+1/2, l_y'+1/2}(\cos 2\alpha) N_{K''}^{l_x' l_y'} (\sin \alpha)^{l_x'} (\cos \alpha)^{l_y'} P_{(K''-l_x'-l_y')/2}^{l_x'+1/2, l_y'+1/2}(\cos 2\alpha). \tag{8}$$

In these expressions, γ refers to the set $\{LSl_xl_y\}$, $a_{ijk} = [A_iA_jA_k/(A_i+A_j+A_k)]^{3/2}$, and A_i is the mass number of constituent i. To calculate spatial densities in another coordinate system (for example in the **Y** system, going from the initial **T** system), we just transform the coordinate parts of the WFs via Raynal-Revai coefficients [28], which rotate the hyperangular part of the WF, conserving the total angular moment L and hypermoment K. After this rotation we calculate spatial densities with new hyperradial WFs, which are superpositions of those calculated in the initial (usually **T**) system.

Most interesting are the correlated densities at resonance energies, and at energies corresponding to peaks in response functions. In the vicinity of narrow resonances, the WF in the interior ($\rho < \rho_0$) can be represented in the factorized form of Eq. (2).

In case of wide resonances, where the interior part of the WF is not so pronounced, and for specific states like the soft modes, the spatial correlations (or anticorrelations) can be filtered by subtracting the APW density (A4) from the full correlated density using Eq. (8). The APW density is thus used as a reference frame. We have seen in Sec. II A how the integral of this difference gives a time delay which coincides with the lifetime for narrow resonances, and is a measure of the ability of interactions to accumulate probability in the interior region.

We shall demonstrate different types of spatial correlations in the ^{6}He three-body continuum, using both "cluster" **T**-basis $(nn)\alpha$ and "quasi-shell-model" **Y**-basis $n(n\alpha)$ Jacobi coordinate representations.

III. RESULTS

All calculations for ^{6}He continuum spatial densities are performed with the modified SBB $\alpha-n$ interaction using soft Pauli core in s wave and the realistic soft core GPT $n-n$ potential (see Ref. [2] for details).

A. Spatial densities for antisymmetrized plane waves

Since the product $(\kappa\rho)$ is the argument of the hyperradial Bessel functions $J_{K+2}(\kappa\rho)$ in the expansion of the six-dimensional APW in Eqs. (A1) and (A4), we can expect an approximate peak position of the spatial density (from the corresponding term) will grow linearly in K as $\kappa\rho_0 \sim (K+2)$. So in polar (ρ,α) coordinates, the density behaves as the square of a Bessel function of integer index $(K+2)$ in ρ, modulated by Jacobi polynomials in α arcs. If we separate the spin components $S=0$ and $S=1$, then correlations will be more clear, bringing additional gaps in α arcs, because the APW density would include only even (odd) angular momenta between the halo neutrons.

The upper plots in Fig. 1 show the spatial densities of the 2^+ partial component of the APW in both coordinate systems.

The densities were computed for the energy $E=1.19$ MeV, corresponding to the 2_1^+ resonance position in ^{6}He calculations performed with a bare $n-\alpha$ interaction with $K_{max}=8$. In both plots one can see the expected oscillating behavior of the APW densities with rather broad peaks close to origin, looking similar in both coordinate representations. The difference in inclination angles for the trajectories of the maxima of APW "waves" ($\pi/4$ for both **T** and **Y** systems in hyperradius and hyperangle coordinates) is due to the difference in the ratio of reduced masses of (ij) and $(ij)k$ subsystems, namely, $\tan\beta = (1+A_c)/\sqrt{A_c(2+A_c)}$ for **Y** basis (β is counted from r_{c-n} axis) and $\tan\beta = \sqrt{2+A_c}/2\sqrt{A_c}$ for **T** (β is counted from r_{n-n} axis). In case of a heavy core and two nucleons we get an angle of $\mathrm{atan}(1/2)$ for the **T** basis and $\pi/4$ for **Y**. In spite of the complex structure of the APW density, which is a square modulus of a coherent sum of K terms with alternating signs of Bessel functions $\Sigma(-1)^{\mathrm{int}(K/2)}J_{K+2}(\kappa\rho)\phi_{Kl_xl_y}(\alpha)$ weighted with the hyperangular part $\phi_{Kl_xl_y}(\alpha)$ of $\mathcal{Y}_{KLM_L}^{l_xl_y}(\Omega_5^\rho)$, see Eq. (A2), and incoherent in S,l_x,l_y (as a result of summation and integration), the asymptotic structure reveals pronounced minima in hyperradial arcs $\sim\sin^2(\kappa\rho_0)/\rho$ (elliptic in r_{ij} and $r_{(ij)-k}$ coordinates) which are mostly due to the destructive interference in the K summation.

The plots show that the positions of the first maxima are situated at $r_{\alpha n}, r_{(\alpha n)n} \sim 25$ fm and $r_{nn} \sim 30$ fm and $r_{(nn)\alpha} \sim 20$ fm. Note that the shifted position of the wide **T** peak is due to more mass "asymmetry" for this system, but that the more stretched shape is because it consists of a sum of three dominating HH with $(KLSl_xl_y) = (22002)$, (22020), (21111) having the different maxima positions in hyperangle, while in the **T** basis the peak is sharper due to a unique dominating structure $(KLSl_xl_y) = (21111)$ (corresponding to the p-shell structure of a 2^+ state). The spatial densities for the 1^- and 0^+ partial components of the APW have similar structure, but with first peak closer to the origin (at the same energy) because of lower index of the Bessel functions.

B. Correlated spatial densities for narrow resonances

To illustrate the correlated spatial density to be expected for a narrow true three-body resonance, we have performed HH calculations for the well-known narrow 2_1^+ resonance in ^{6}He at 0.83 MeV above the three-body threshold. Since the lowest components with hypermoment $K=2$ gives about 95% of the internal norm, the calculations used $K_{max}=8$, which results in a resonant energy of 1.19 MeV, but with almost the same geometrical structure of the internal part of the WF. The results are shown in the lower part of Fig. 1 for both **T** and **Y** Jacobi coordinate systems.

These densities are spatially focused (note the different radial scales of upper and lower plots in Fig. 1) and have properties similar to a bound state. The spatial densities are uniquely characterized by having only one pronounced peak with maximum (most probable position) at $r_{nn} \sim 5$ fm, $r_{(nn)\alpha} \sim 3$ fm, and $r_{\alpha n} \sim r_{(\alpha n)n} \sim 3.5$ fm, i.e., at short dis–
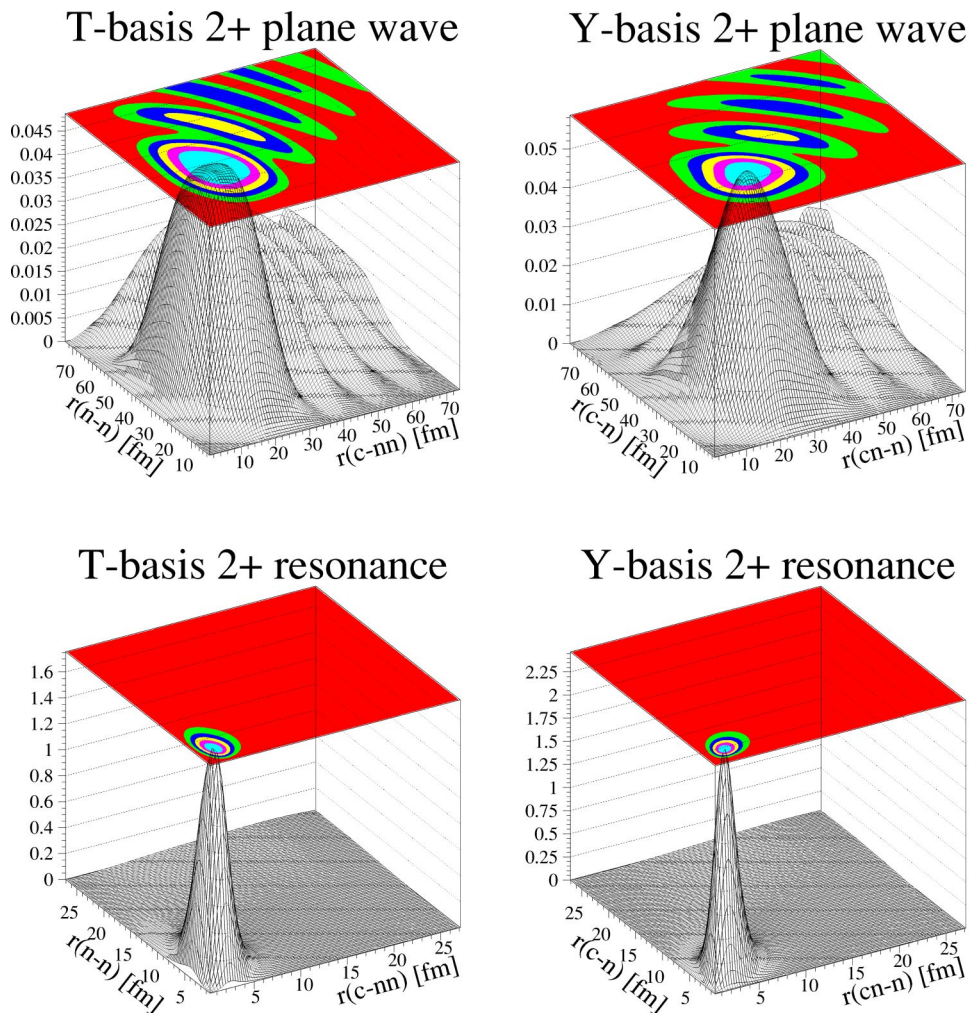
FIG. 1. (Color online) Spatial correlations for the 2^+ partial component of an APW (upper row) and the 2_1^+ resonance calculated at resonant energy $E = 1.19$ MeV in **T** and **Y** coordinate systems.

tances, compared with the first prominent peak ∼25 fm corresponding to the APW. The 2_1^+ resonance has properties of a quasistationary state with characteristic r.m.s. hyperradius of about 11 fm, matter radius $r_{mat} \sim 4.8$ fm, and r.m.s. distance between valence neutrons and between a valence neutron and core of ∼10 fm, calculated as a quasibound state with exponentially decreasing asymptotics.

The magnitude of correlations inside the interaction region is three orders of magnitude larger than that of the large-distance background (which is not visible on the scale of the corresponding spatial densities in Fig. 1). Note that the internal WF almost coincides with the quasibound state that would be found by using a boundary condition of an exponentially decreasing tail at the same *positive* energy. This is in correspondence with the general results for quasistationary states [29].

C. Correlated spatial densities for broad resonances

Correlated spatial densities for broad three-body resonances are essentially more complicated than for narrow ones. To illustrate the effects which can be expected for broad structures we studied the correlated spatial densities for the second 2^+ and first 1^+ resonances in ^{6}He [2]. Correlation plots for the 2_2^+ resonance at 3.6 MeV are presented in

the upper part of Fig. 2 for both **T** and **Y** systems. They exhibit structure characterized by absence of strong concentration of density in the interaction region of all three particles. The characteristic features of these densities are two pronounced peaks, one at $r_{nn} \sim 5$ fm, $r_{(nn)\alpha} \sim 3$ fm, $r_{\alpha n} \sim r_{(\alpha n)n} \sim 3$ fm in, respectively, **T** and **Y**, which may correspond to attraction in the region of joint interaction of all three particles, and a second peak at $r_{nn}, r_{(nn)\alpha} \sim r_{\alpha n}, r_{(\alpha n)n} \sim 12$ fm, positioned almost at the first APW peak, calculated at the same energy. To obtain additional information about the real correlations we have subtracted the spatial density for the APW from the calculated correlated density for the 2_2^+ resonance (upper part of Fig. 2). The results are shown in the lower part of Fig. 2 again for both **T** and **Y** systems. In these plots one can easily see that only the first peak survives after the subtraction, which filters out the real resonant part of corresponding density.

The remaining peak (lower part of Fig. 2) in both **T** and **Y** is about five times larger than the residual "background" and is situated, as is the first 2^+ resonance, in the region where all three particles are interacting. This situation is specific for above-barrier resonances, where the WFs have only moderate amplifications in the internal region. After subtraction the background has regular structure around the first maximum, followed by a wavelike sequence with minima at asymptotic
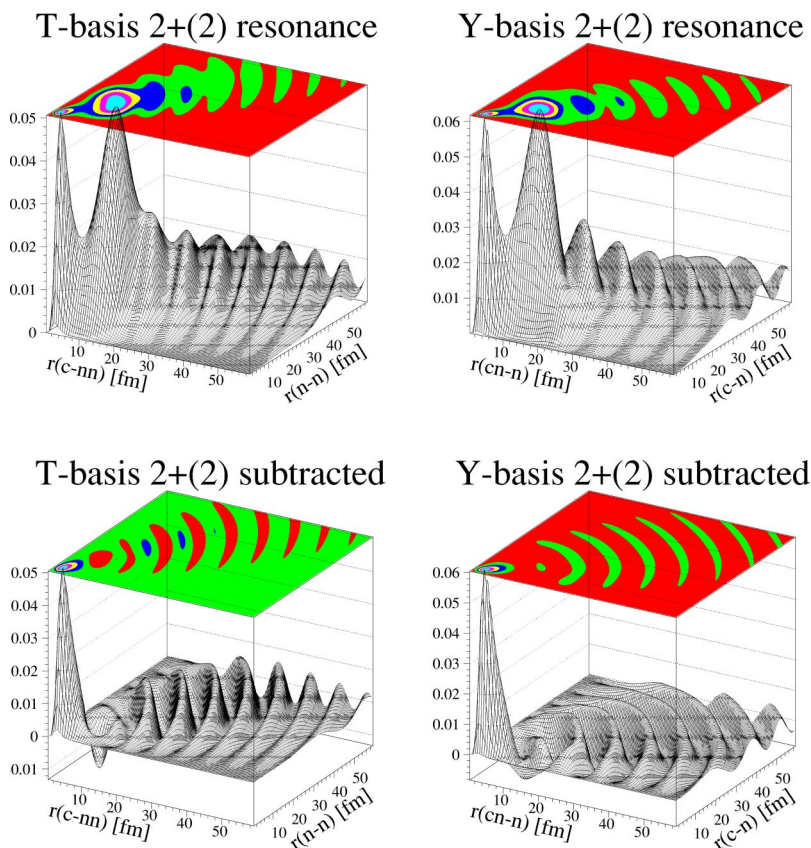
FIG. 2. (Color online) Spatial correlations for the 2_2^+ resonance (upper row) and with subtracted nn APW (lower row) at energy 3.6 MeV in **T** and **Y** systems.

distances which are negative due to the significant phase shift between the scattered and plane waves (see contour plot on top of Fig. 2).

Results similar to that of the 2_2^+ resonance are found for the 1_1^+ resonance, which can also be classified as an above-barrier resonance.

Correlated spatial densities for three-body virtual-like excitations

In spite of the presence [2] of a 1^- soft dipole resonance-like peak in both nuclear and electromagnetic response functions at ~ 1.5 MeV, the correlated spatial density plot, shown in Fig. 3, shows lack of noticeable resonant behavior in the interior region, but strongly peaked structures at $r_{nn}, r_{(nn)\alpha} \sim r_{\alpha n}, r_{(\alpha n)n} \sim 15-20$ fm.

Subtraction of the APW density leaves only a 25% difference in magnitude in the interior region ~ 5 fm, and comparable background until distances ~ 50 fm. In comparison with the 2_2^+ case there are irregular structures along the arcs within distances ~ 30 fm. These structures have different character in **T** and **Y** systems and resemble the large scale ~ 25 fm spatial APW correlations. A small peak in the interior region (at about 4 fm) may look like an above-barrier resonance (2_2^+ and 1_1^+ cases), but is hardly prominent enough to justify classification as a resonant state taking into account the comparable background.

In Ref. [2] we analyzed the soft dipole mode in ^{6}He, which might be a barrier-top resonance because of the generally repulsive character of the averaged interaction between the three particles plus centrifugal barrier. We found

however no resonance but a virtual-state-like behavior of eigenphases, along with a bump in the nuclear and EM dipole strength functions. It could be a coupled-channels type resonance created by distributed coupling between the channels in absence of deep diagonal potentials. However, the lowest term in the diagonalized potential matrix plus centrifugal barrier shows repulsion, with a very small pocket not deep enough to produce an above-barrier wide resonance [2]. The characteristic feature of a barrier-top resonance in the two-body case is a small resonance peak in the elastic cross section, while the interior norm exhibits sharp resonant behavior [19], and these features should be the same in the three-body case. Here, however, for the 1^- the calculated interior norm has no resonant behavior [2], only a monotonic increase with energy. The lesson from the spatial correlations adds consistently to this picture.

Figure 4 presents the correlated density plot for the 0^+ monopole continuum at the peak energy $E=1.8$ MeV of the monopole response. Like in the 1^- case there are strong peaks at distances $\sim 25-30$ fm and a remnant of the ground state dineutron and cigar configurations [3] located close to the origin. Subtraction of the APW density "kills" 50% of their magnitude, but leave the irregular arc structure in this region, which can be attributed with monopole continuum correlations. Figure 4 demonstrates also a lack of resonant behavior in the interior region. The large scale of continuum correlations after subtraction of the APW density can be seen from a comparison with the remnant of the halo ground-state dineutron and cigar configurations.

The monopole response function (not shown) has a wide bump covering the possible energy locations for both soft
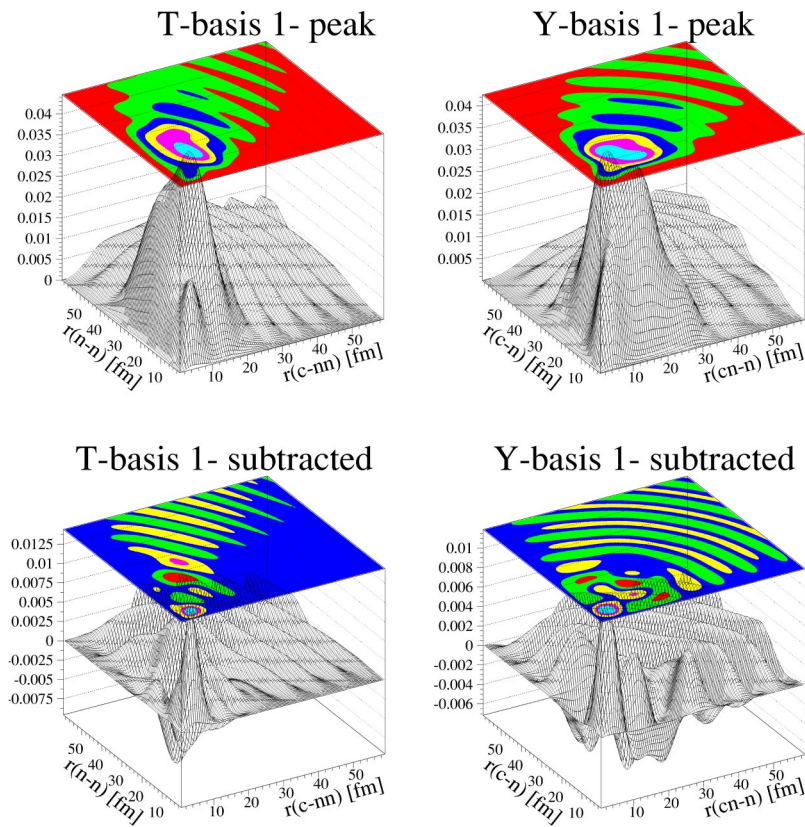
FIG. 3. (Color online) Spatial correlations for the energy peak position of the 1^- soft dipole mode (upper row) and after subtraction of the APW density (lower row) in **T** and **Y** systems.
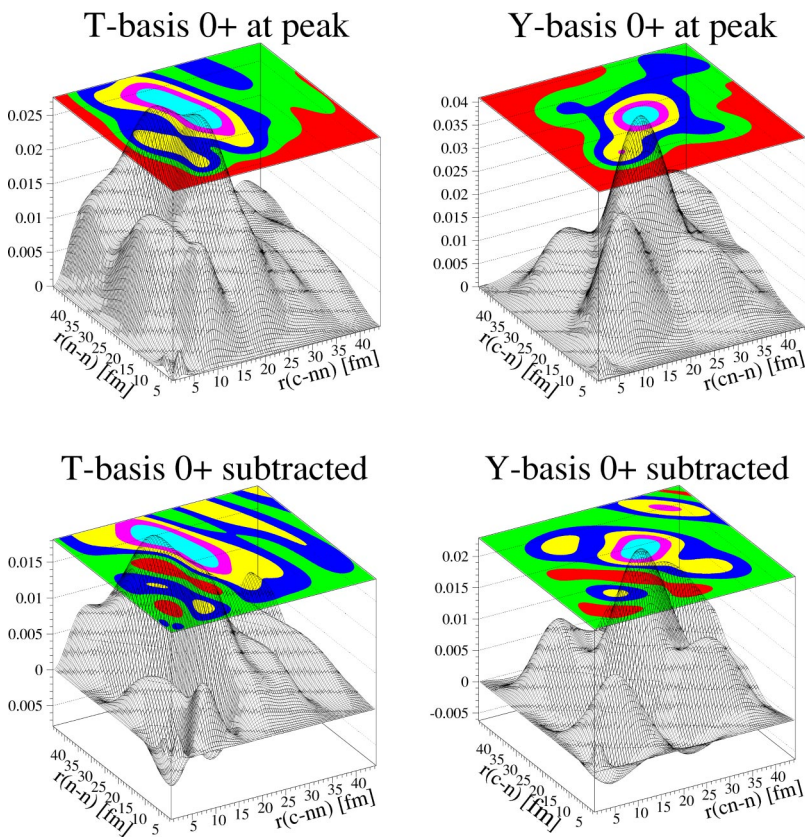

FIG. 4. (Color online) Spatial correlations for the energy peak position of the 0^+ soft monopole mode (upper row) and after subtraction of the APW density (lower row) in **T** and **Y** systems.

monopole breathing and spin-flip modes [2]. With this motivation we performed calculations at energies $E=0.8$ MeV and $E=5.0$ MeV, which are below and above than the expected peak position. The findings are quite similar to those discussed above. There are only long-range correlations but no resonance structure. Taking into account the predominant s-wave decay of the 0^+ state via a correlated pair of neutrons at low energy, and the p-wave decay via ^{5}He resonance at higher energies, as well as strong mixing of these modes, we may conclude that these modes are unavoidably spread in the three-body continuum.

We therefore need further analysis of this important mode, which could give valuable information about the compression modulus of a dilute "neutron gas" which could be associated with the halo neutrons, and, in principle, could be extracted from the energy position of the monopole breathing mode. Such perspectives are even more relevant for ^{8}He.

IV. DISCUSSION AND CONCLUSIONS

The developments of the hyperspherical harmonics method have deepened and enriched the understanding of the Borromean three-body continuum. Using the example of ^{6}He as a testbench we have analyzed several interesting continuum structures using both the Jacobian cluster **T** basis and the translationally invariant shell-model **Y** basis. The continuum information is derived from the spatial correlated densities, which also previously proved to be very useful in understanding the ground state of ^{6}He [3].

The 2_1^+ state of ^{6}He is a true three-body Borromean resonance with characteristic features: (i) a narrow width and (ii) a strong concentration of the WF in the internal region where all three particles are interacting close to each other. As a consequence, the hyperradial WF in the interaction region has the characteristic resonance amplification, for 2_1^+ three orders of magnitude larger than the antisymmetrized plane wave amplitude, and with an energy dependence which coincides with the energy dependence of the three-body scattering amplitude.

The 2_2^+ and 1_1^+ resonant states in ^{6}He are wide above-barrier resonances, produced by the generally attractive averaged interactions, but with no pronounced concentration of density in the interior region even after filtering out the nonresonant background coming from plane waves.

We also find some wide above-barrier resonance candidates which are completely spread into the continuum. In the 0^+ continuum of ^{6}He, at least two states should exist, orthogonal to the ground state: the soft monopole breathing and spin-flip modes [2]. Our previous analysis in Ref. [2] showed nonresonant behavior, although the response function exhibits a wide peak at 1.8 MeV. The correlated spatial density for 0^+ at this energy has a peaked structure in the region inside 30 fm, but after subtracting the density for plane waves, only half the density remains, revealing long-range correlations, but no concentration of density in the internal region. Perhaps this is a characteristic feature of any monopole three-body continuum, where there is a possibility for s-wave decay via the virtual s-wave state of the two halo neutrons.

There are also peaks in the response functions for soft modes, which have tentatively been related to large induced multipole moments. In Ref. [2] we analyzed the 1^- soft dipole mode in ^{6}He, which could be a barrier-top resonance because of the generally repulsive character of the averaged interaction between three particles. We found however no resonance but a virtual-state-like behavior of eigenphases, along with a bump in dipole strength functions. The present study of the corresponding 1^- correlated spatial densities at the peak position shows (after subtraction of the plane wave density) that only a quarter of the dipole density remains, along with long-range correlations (at about 30 fm) analogous to the monopole continuum structure. A small peak in the interior region (at about 4 fm) resembles the above-barrier resonances (like in the 2_2^+ and 1_1^+ cases), but is not enough pronounced to justify classification as a resonant state. Neither it is a coupled-channels type resonance created by distributed coupling between the channels in absence of deep diagonal potentials. Since the lowest term in the diagonalized potential matrix shows repulsion, with a very small pocket not deep enough to produce a wide above-barrier resonance [2]. The characteristic feature of a barrier-top resonance in the two-body case is a small resonance peak in the elastic cross section, while the interior norm exhibits a sharp resonant behavior [19], and these features should be the same in three-body case. Here, however, the calculated interior norm has no resonant behavior [2], only a monotonic increase with energy.

The monopole and dipole continuum of ^{6}He illustrate specific states which may be classified as Efimov-like continuum structures near the three-body threshold. In physical analogy with the bound state Efimov effect, the origin of these states are the long-range effective three-body interactions with a range of the order of the sum of the scattering lengths in the binary subsystems. There is then a large correlation distance, and no concentration of the WF inside the region of interaction of all particles, only a long-range spreading of correlations. However, we need further explorations of these states in terms of energy correlations in three-body continuum to distinguish between the decay through resonances in two-body subsystems and Efimov-like states; this is the subject of forthcoming publication.

The spatial correlations shown here depend on the analytical properties of wave functions and scattering amplitudes, and enable as we have tried to demonstrate more reliable conclusions about resonant or nonresonant nature of such challenging cases as the soft dipole mode.

APPENDIX: THREE-BODY COORDINATES AND CONTINUUM

Normalized Jacobi coordinates $(\mathbf{x}_k, \mathbf{y}_k)$ which are used in construction of the HH basis [2,3] are colinear with natural

coordinates $(\mathbf{r}_{ij}, \mathbf{r}_{(ij)k})$ corresponding to the distance between any two particles and between their center of mass and a third one. We use the designation for coordinate systems: cluster **T** basis with $x \sim r_{nn}$ (with corresponding wave number $\mathbf{k}_x$) and $y \sim r_{(nn)-core}$ (with corresponding $\mathbf{k}_y$), and quasi-shell-model **Y** basis with $x \sim r_{core-n}$ and $y \sim r_{(core-n)-n}$ coordinates. Let us consider two nucleons of unit mass outside a core of mass A. We first transform from Cartesian coordinates $|\mathbf{x}|$, $|\mathbf{y}|$ to polar coordinates— hyperradius $\rho = \sqrt{x^2 + y^2} = \sqrt{\frac{1}{2}r_{nn}^2 + 2A/(2+A)r_{(nn)-core}^2} = \sqrt{A/(1+A)r_{core-n}^2 + (1+A)/(2+A)r_{(core-n)-n}^2}$ and hyperangle $\alpha = \mathrm{atan}(x/y)$, joined into five rotational degrees of freedom—the hyperangle α and the usual angles defined by the directions $\hat{\mathbf{x}}$ and $\hat{\mathbf{y}}$. In the same way it is possible to

define hyperspherical coordinates in momentum space: transform from Cartesian wave numbers $|\mathbf{k_x}|$, $|\mathbf{k_y}|$ to polar hyper-momentum $\kappa = \sqrt{k_x^2 + k_y^2} = \sqrt{2mE/\hbar^2}$ and corresponding hyper-angle $\alpha_\kappa = \mathrm{atan}(k_x/k_y)$, combined with four rotational degrees of freedom which are angles $\hat{\mathbf{k_x}}$ and $\hat{\mathbf{k_y}}$. In the expression for κ, m is a scaling nucleon mass, and E is the total energy calculated from three-body threshold.

The plane wave is the continuum reference state, by comparison with which we introduce the phase shifts, as a measure of the scattering ability of the interaction potentials. In the two-body case the phase shift is defined for radial motion and the plane wave is expanded in spherical harmonics. The three-body plane wave allows equivalent representation in the HH basis. For spinless particles the six-dimensional plane wave in any Jacobi system is

$$
\begin{aligned}
(2\pi)^{-3}\exp\left[i(\mathbf{k_x}\cdot\mathbf{x} + \mathbf{k_y}\cdot\mathbf{y})\right] &= (\kappa\rho)^{-2}\sum_{KLM_L l_x l_y} i^K J_{K+2}(\kappa\rho)\mathcal{Y}^{l_x l_y}_{KLM_L}(\Omega_5^\rho)[\mathcal{Y}^{l_x l_y}_{KLM_L}(\Omega_5^\kappa)]^* \\
&= (\kappa\rho)^{-5/2}\sum_{KLl_x l_y}\Psi^L_{Kl_x l_y}(\kappa\rho)\mathcal{Y}^{l_x l_y}_{KLM_L}(\Omega_5^\rho)[\mathcal{Y}^{l_x l_y}_{KLM_L}(\Omega_5^\kappa)]^*,
\end{aligned} \tag{A1}
$$

which we use to define $\Psi^L_{Kl_x l_y}(\kappa\rho)$ in terms of Bessel functions J_{K+2} of integer index. The five-dimensional angular function $\mathcal{Y}^{l_x l_y}_{KLM_L}(\Omega_5^\rho)$ is expressed in terms of spherical functions Y_{lm} in $\hat{\mathbf{x}}$, $\hat{\mathbf{y}}$ and Jacobi polynomials $P^{l_x+1/2,l_y+1/2}_{K-l_x-l_y/2}(\cos 2\alpha)$ carrying hyperangular momentum K, and with the explicit form

$$
\begin{aligned}
\mathcal{Y}^{l_x l_y}_{KLM}(\Omega_5) = N^{l_x l_y}_K(\sin\alpha)^{l_x}(\cos\alpha)^{l_y}P^{l_x+1/2,l_y+1/2}_{K-l_x-l_y/2}(\cos 2\alpha)[Y_{l_x}(\hat{\mathbf{x}}) \\
\otimes Y_{l_y}(\hat{\mathbf{y}})]_{LM}.
\end{aligned} \tag{A2}
$$

For Borromean halo nuclei we have to take into account spins of valence neutrons and the antisymmetrization of the wave function under exchange of valence neutrons. The simplest way to treat antisymmetrization between halo neutrons is constructing the channels in the **T**-basis set with $x \sim r_{nn}$. Thus the antisymmetrization can then be included by imposing $\{l_x + S + T = \mathrm{odd}\}$, where l_x is the relative orbital angular momentum between the two neutrons, S and $T = 1$ are the total spin and isospin of the two-neutron subsystem. This means that the even l_x are combined with $S = 0$, while odd l_x are combined with $S = 1$ only. Effective antisymmetrization between halo neutron and the core is realized on a dynamical level by including a Pauli repulsive core in those partial components of the N-core interaction, where corresponding N-core states are forbidden by the Pauli principle, or by excluding those states dynamically from the three-body solutions [4].

We seek our bound state and continuum wave functions in the form of an expansion on generalized angle-spin basis keeping antisymmetrization between halo neutrons

$$
\Upsilon^{K\gamma}_{JM}(\Omega_5) = \hat{A}_{nn}[\mathcal{Y}^{l_x l_y}_{KL}(\Omega_5) \otimes X_S]_{JM}, \tag{A3}
$$

where $\hat{A}_{nn}$ is antisymmetrizer, and the γ index refers to the quantum number set $\{LSl_x l_y\}$. The corresponding plane wave (A1) has to include also the fermionic nature of the halo nucleons for isospin T, and can be represented as a sum over total momenta JM components $\Upsilon^{K\gamma}_{JM}(\Omega_5)$,

$$
\begin{aligned}
\Phi^T_{\kappa JM}(\mathbf{x},\mathbf{y},\hat{\mathbf{k}}_x,\hat{\mathbf{k}}_y,\alpha_\kappa) &= (\kappa\rho)^{-5/2}\sum_{K\gamma}\Psi^L_{Kl_x l_y}(\kappa\rho)\Upsilon^{K\gamma}_{JM}(\Omega_5^\rho) \\
&\times \sum_{M_L M_S}\langle LM_L SM_S|JM\rangle\mathcal{Y}^{l_x l_y}_{KLM_L}(\Omega_5^\kappa)X_T
\end{aligned} \tag{A4}
$$

with $\Psi^L_{Kl_x l_y}$ defined above.

For continuum states in the presence of interaction potentials, the general solution of the coupled-channel problem for given JM is the wave function

$$
\begin{aligned}
\boldsymbol{\Psi}^T_{\kappa JM}(\mathbf{x},\mathbf{y},\hat{\mathbf{k}}_x,\hat{\mathbf{k}}_y,\alpha_\kappa) \\
= (\kappa\rho)^{-5/2}\sum_{K\gamma,K'\gamma'}\psi^J_{K\gamma,K'\gamma'}(\kappa\rho)\Upsilon^{K\gamma}_{JM}(\Omega_5^\rho) \\
\times \sum_{M'_L M'_S}\langle L'M'_L S'M'_S|JM\rangle\mathcal{Y}^{l'_x l'_y}_{K'L'M'_L}(\Omega_5^\kappa)X_T. \tag{A5}
\end{aligned}
$$

Hyperradial functions in Eqs. (A4) and (A5) for each JM are normalized in the same way

$$\int \boldsymbol{\Psi}_{\kappa'}^{*} \boldsymbol{\Psi}_{\kappa} \rho^5 d\rho = \kappa^{-5} \delta(\kappa' - \kappa). \tag{A6}$$

After separation of angle-spin parts in the Schrödinger equation, the three-body problem is reduced to a system of hyperradial equations treating on equal footing both for the bound state and three-body continuum. Asymptotically, the continuum wave function has a form (familiar from two-body scattering)

$$\sum_{JM} \Psi_{\kappa JM}^{T}(\mathbf{x},\mathbf{y},\hat{\mathbf{k}}_{x},\hat{\mathbf{k}}_{y},\alpha_{\kappa}) \sim_{\rho \to \infty} \left[\exp[i(\mathbf{k_x} \cdot \mathbf{x} + \mathbf{k_y} \cdot \mathbf{y})] \right.$$

$$\left. + A(E,\Omega_5^{\rho},\Omega_5^{\kappa}) \frac{\exp(i\kappa\rho)}{(\kappa\rho)^{5/2}} \right] X_S X_T, \tag{A7}$$

where $(\kappa\rho)^{-5/2}e^{i\kappa\rho}$ is now the outgoing three-body spherical wave with $3 \to 3$ scattering amplitude $A(E,\Omega_5^{\rho},\Omega_5^{\kappa})$.

[1] B. V. Danilin and M. V. Zhukov, Phys. At. Nucl. **56**, 460 (1993); B. V. Danilin *et al.*, Few-Body Syst., Suppl. **10**, 273 (1999).

[2] B. V. Danilin, I. J. Thompson, M. V. Zhukov, and J. S. Vaagen, Nucl. Phys. **A632**, 383 (1998).

[3] M. V. Zhukov B. V. Danilin, D. V. Fedorov, J. M. Bang, I. J. Thompson, and J. S. Vaagen, Phys. Rep. **231**, 151 (1993).

[4] I. J. Thompson, B. V. Danilin, V. D. Efros, J. S. Vaagen, J. M. Bang, and M. V. Zhukov, Phys. Rev. C **61**, 024318 (2000).

[5] E. Garrido, D. V. Fedorov, and A. S. Jensen, Nucl. Phys. **A617**, 153 (1997).

[6] B. V. Danilin, Izv. Akad. Nauk SSSR, Ser. Fiz. **54**, 2212 (1990).

[7] A. Csótó, Phys. Rev. C **49**, 3035 (1994).

[8] T. Myo, K. Kato, S. Aoyama, and K. Ikeda, Phys. Rev. C **63**, 054313 (2001).

[9] G. F. Filippov *et al.*, Prog. Theor. Phys. **96**, 575 (1996); J. Math. Phys. **36**, 4571 (1995).

[10] S. A. Zaitsev, Y. F. Smirnov, and A. M. Shirokov, Theor. Math. Phys. **117**, 1291 (1998); Yu. A. Lurie and A. M. Shirokov, Bull. Russ. Acad. Sci. Phys. **61**, 1665 (1997).

[11] V. I. Kukulin *et al.*, Sov. J. Nucl. Phys. **29**, 421 (1979); N. Tanaka, Y. Suzuki, and K. Varga, Phys. Rev. C **56**, 562 (1997).

[12] S. N. Ershov *et al.*, Phys. Rev. C **56**, 1483 (1997); S. N. Ershov, B. V. Danilin, and J. S. Vaagen, *ibid.* **64**, 064609 (2001).

[13] T. Aumann *et al.*, Phys. Rev. C **59**, 1252 (1999).

[14] B. Jonson, Phys. Rep. **389**, 1 (2004).

[15] I. Tanihata, J. Phys. G **22**, 157 (1996).

[16] P. G. Hansen *et al.*, Annu. Rev. Nucl. Part. Sci. **45**, 591 (1995).

[17] V. M. Efimov, Comments Nucl. Part. Phys. **19**, 271 (1990).

[18] W. Greiner, in *Resonances in Heavy Ion Reactions*, edited by K. A. Eberhard, Lecture Notes in Physics Vol. 156 (Springer-Verlag, Berlin, 1982), p. 415.

[19] S. Fluegge, *Practical Quantum Mechanics* (Springer-Verlag, Berlin, 1971), ISBN: 3540650350.

[20] I. R. Afnan, Aust. J. Phys. **44**, 201 (1991).

[21] A. I. Baz' and S. P. Merkuriev, Theor. Math. Phys. **70**, 397 (1976).

[22] N. B. Shulgina and B. V. Danilin, Nucl. Phys. **A554**, 137 (1993).

[23] H. C. Ohanian and C. G. Ginsburg, Am. J. Phys. **42**, 310 (1974).

[24] A. I. Baz', Zh. Eksp. Teor. Fiz. **70**, 397 (1976).

[25] A. M. Badalyan, L. P. Kok, M. I. Polikarpov, and Yu. A. Simonov, Phys. Rep. **82**, 31 (1982).

[26] V. I. Kukulin, V. M. Krasnopolsky, V. I. Voronchev, and P. B. Sazonov, Nucl. Phys. **A453**, 365 (1986).

[27] B. V. Danilin, M. V. Zhukov, A. A. Korsheninnikov, L. V. Chulkov, and V. D. Efros, Sov. J. Nucl. Phys. **48**, 1208 (1988).

[28] J. Raynal and J. Revai, Nuovo Cimento A **A68**, 612 (1970).

[29] A. I. Baz', Ya. B. Zel'dovitch, and A. M. Perelomov, *Scattering, Reactions and Decay in Non-relativistic Quantum Mechanics* (Moscow, Nauka, 1971), Translated from Russian, Israel Program for Scientific Translations, Jerusalem, 1969.